



# Effect of thermal stresses on the microstructure of the continuous cooling TiAl alloys



Bin Zhu<sup>a</sup>, Xiangyi Xue<sup>a</sup>, Hongchao Kou<sup>a,b,\*</sup>, Bin Tang<sup>a</sup>, Jinshan Li<sup>a,b</sup>

<sup>a</sup> State Key Laboratory of Solidification Processing, Northwestern Polytechnical University, Xi'an, 710072, China

<sup>b</sup> National & Local Joint Engineering Research Center for Precision Thermal-forming Technology of Advanced Metal Materials, Xi'an, 710072, China

## ARTICLE INFO

### Keywords:

Titanium aluminides  
Thermal stresses  
 $\gamma$  variants  
LAGBs  
Dislocations  
Thermal-induced deformation

## ABSTRACT

A series of continuous cooling tests were performed on TiAl alloys using a Gleeble3500 machine to investigate the effect of thermal stresses on the microstructure. The results show that macroscopic thermal stresses promote correlated nucleation of  $\gamma$  lamellae. The trend of the dominance of one twin-group  $\gamma$  variants in local regions is weakened, and the  $\gamma/\gamma$  interfaces tend to be true twin and pseudotwin boundaries rather than  $120^\circ$  rotational faults under macroscopic thermal stresses. Meanwhile, thermal-induced deformation generated under the effect of both microscopic and macroscopic thermal stresses results in numerous low angle grain boundaries (LAGBs) and dislocations. The LAGBs and dislocations distribute heterogeneously among lamellar colonies and phases. No mechanical twins are observed due to the low strain and low strain rate characteristics of the thermal-induced deformation. These findings could shed light on understanding and preventing the cracking of TiAl components during cooling process.

## 1. Introduction

TiAl alloys have been successfully utilized for high-temperature components in aerospace and automotive industries after decades of R & D activities [1–3]. In recent years, a large part of scientific work has been dedicated to TiAl alloys with a high content of  $\beta$ -stabilizing elements, such as Nb and Mo, for improving the service temperature and hot workability [4–6]. However, the extreme brittleness in the as-cast condition along with the high thermal stresses generated during the cooling process make casting and melting of such alloys challenging due to the high propensity for cold cracking [7,8].

During the cooling process of TiAl components, the appearance of high temperature gradients results in inhomogeneous contraction at different parts, and lead to macroscopic thermal stresses. Additionally, the mismatch of thermal expansion coefficients of different phases causes microscopic thermal stresses in the vicinity of phase boundaries [9]. A lot of simulations have been done to study the building up of macroscopic thermal stresses of TiAl ingots and castings for solving the cracking [8,10,11]. Nevertheless, the effect of thermal stresses on the microstructure of TiAl alloys has not been investigated, which is of great importance for understanding the cracking.

Phase transformation and thermal-induced deformation occur simultaneously during the cooling process. During the lamellar transformation, the  $\gamma$  lamellae are formed in  $\alpha$  grain following the

orientation relationship of  $\{111\}_{\gamma}/\{0001\}_{\alpha}$  and  $\langle 1-10 \rangle_{\gamma}/\langle 11-20 \rangle_{\alpha}$  [12]. Six different  $\gamma$  variants are formed due to the tetragonality of the  $\gamma$  phase. The variants are separated into two twin groups with opposite stacking sequences of  $\{111\}$  plane and three types of lamellar boundaries are formed between different  $\gamma$  variants, i.e., twin, pseudo-twin, and ordered-domain boundaries. It has been illustrated that the distributions of  $\gamma$  variants and  $\gamma/\gamma$  interfaces are determined by the nucleation and growth at different stages of the lamellar transformation [13,14]. The phase field simulations showed that external stresses can influence  $\gamma$  nucleation during  $\alpha \rightarrow \gamma + \alpha_2$  phase transformation, and thus change twin boundary fractions [15,16]. Meanwhile, it has been demonstrated that the heterogeneous distribution of dislocations and twin interactions are intimately related to the microcracking of TiAl alloys [17–19]. Therefore, it's of great importance to investigate the characteristics of the lamellar structure and deformation substructures of TiAl alloys cooled under thermal stresses.

In this study, a series of physical vacuum arc remelting (VAR) simulations were performed on specimens of TiAl alloys using a Gleeble3500 machine. The specimens were subjected to thermal and stressing histories similar to those experienced by material points of TiAl ingots during cooling process. Then, the microstructures were analyzed for determining the effect of thermal stresses on the microstructure of TiAl alloys.

\* Corresponding author. State Key Laboratory of Solidification Processing, Northwestern Polytechnical University, Xi'an, 710072, China.  
E-mail address: [hchkou@nwpu.edu.cn](mailto:hchkou@nwpu.edu.cn) (H. Kou).

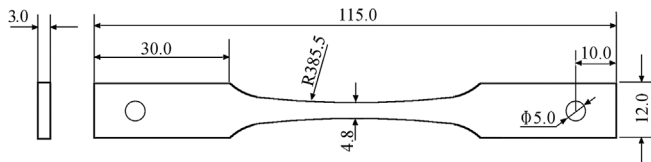


Fig. 1. Geometry of a tensile specimen used for continuous cooling tests on Gleeble3500 (dimensions in mm).

## 2. Material and experimental

### 2.1. Specimen preparation

The materials used in this study were cut from a VAR ingot with a practical composition of Ti-43.46Al-8.20Nb-0.21W-0.19B-0.28Y (at. %). The ingot was remelted for three times in order to ensure composition homogeneity, and then annealed at 800 °C for 4 h followed by furnace cooling for residual stress relaxation. The flat specimens (Fig. 1) were wired-cut from 1/2 height location of the ingot, with longitudinal direction parallel to the ingot bottom. The central regions of the specimens were slightly curved to ensure the strain concentration. X-ray flaw detection and density measurement were performed after specimen preparation to pick out specimens without solidification defects, such as cavities and inclusions.

### 2.2. Gleeble continuous cooling tests

Three cases of continuous cooling tests denoted by CT<sub>1</sub>, CT<sub>2</sub> and CT<sub>3</sub> were carried out on a Gleeble 3500 thermal-mechanical simulator. As input to the Gleeble experiments, the temperature and tensile stress were set according to the finite element simulation of temperature and macroscopic thermal stresses of a TiAl VAR ingot [8]. The CT<sub>1</sub> specimen was heated and cooled as the temperature curve shown in Fig. 2 without external tensile stress. The specimen was heated to 1320 °C, which is above the  $\gamma$ -solvus temperature for the TiAl alloy [20], and maintained for 60s to eliminate the  $\gamma$  lamellae. Then it was cooled to 1000 °C with a cooling rate of 2 °C/s, and to 25 °C with 1 °C/s in vacuum. The CT<sub>2</sub> specimen was subjected to the same cooling process as CT<sub>1</sub> specimen. Meanwhile, a uniaxial tensile stress equivalent to the maximum principle stress of the most dangerous part for cracking of the VAR ingot was applied during the cooling process. As shown in Fig. 2, the tensile load was applied as the specimen was cooled to 1200 °C, linearly increased to 95 MPa at 1000 °C, and to 380 MPa at 900 °C, then held constantly until room temperature. For CT<sub>3</sub> specimen, the tensile load was removed at 950 °C to investigate the effect of macroscopic thermal stresses on lamellar transformation excluding the possible influence of thermal induced deformation at low temperature on microstructure characterization.

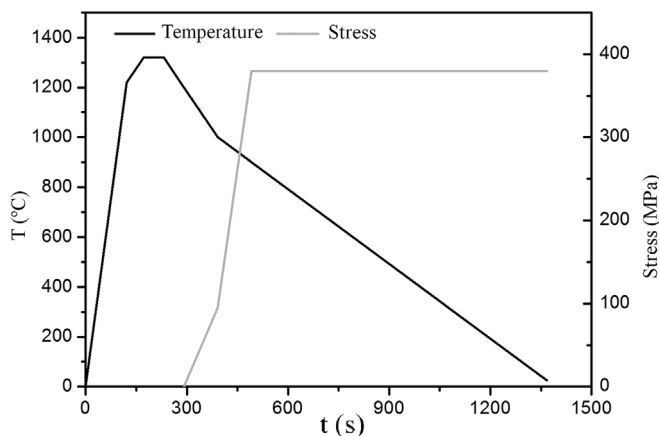


Fig. 2. Temperature and tensile stress curves used in the Gleeble tensile tests.

### 2.3. Microstructure characterization

The microstructures of the raw material and Gleeble tested specimens were characterized by a VEGA II LMH scanning electron microscope (SEM) using the back scattered electron (BSE) mode. The distributions of one-twin-dominant zones (OTDZs) and low angle grain boundaries (LAGBs) were investigated by electron backscatter diffraction (EBSD) on a Tescan MIRA SEM. A small probe size ( $\sim 5$  nm) and a step size of 0.5  $\mu\text{m}$  were used in the EBSD analysis. The  $\gamma$  phase was indexed as generic face-centred cubic structure, while the B2 phase as titanium body-centred cubic. The samples for EBSD investigations were vibratory polished to remove the surface layer. Detailed analyses of  $\gamma$  variants and dislocations were performed on a FEI Tecnai F30 transmission electron microscope (TEM). The samples for TEM analysis were cut perpendicular to the tensile axis and prepared by conventional twin-jet electropolishing. All the samples for microstructure characterization were obtained from the central regions of Gleeble tested specimens.

## 3. Results and discussion

### 3.1. Metallographic microstructure

The metallographic microstructures of the raw material and Gleeble tested specimens are shown in Fig. 3. The TiAl ingot exhibits a near lamellar structure with  $\gamma$  grains (grey contrast) and residual B2 phase (bright contrast) presenting at colony boundaries and triple junctions, as shown in Fig. 3 (a). The white particles are yttrium oxide. The colony size of the raw material is about 50–100  $\mu\text{m}$ . The phase constituents and colony sizes of Gleeble tested specimens are basically the same, as shown in Fig. 3 (b) and (c). Compared with the raw material, the volume fraction of lamellar colonies on CT<sub>1</sub> and CT<sub>2</sub> specimens increase while the ratios of length to width decrease due to the isothermally holding above the  $\gamma$ -solvus temperature. At the same time, the lamellar spacings decrease because of the relatively faster cooling rates during the Gleeble simulations.

### 3.2. The distribution of OTDZs and LAGBs

The orientation mapping and grain boundary distribution of  $\gamma$  major phase for CT<sub>1</sub> and CT<sub>2</sub> specimens are shown in Fig. 4. The  $\beta$ /B2 phase and  $\alpha_2$  phase are in green and yellow separately. The  $\gamma$  lamellae in one colony are indexed into two twin groups with the opposite stacking sequences of  $\{111\}_\gamma$  planes since we assumed a cubic symmetry for  $\gamma$  phase [12]. The bands in lamellar colonies correspond to OTDZs, which generally cover tens of  $\gamma$  lamellae dominated by the variants belonging to one twin group [14], as discussed later in Section 3.3. It is generated due to the preferred nucleation of  $\gamma$  lamellae during  $\alpha \rightarrow \gamma$  transformation, as illustrated previously by other researchers [12,13]. During the cooling process, microscopic thermal stresses were generated in  $\alpha$  phase due to thermal contraction on both CT<sub>1</sub> and CT<sub>2</sub> specimens. The  $\gamma$  lamellae nucleated in favored orientation at  $\alpha$  grain boundaries for minimizing the local elastic energy and resulted in the generation of OTDZs. Since the OTDZs were observed on both CT<sub>1</sub> and CT<sub>2</sub> specimens, and the tensile stress, which represents the macroscopic thermal stresses, was subjected to CT<sub>2</sub> specimen at 1200 °C, it indicates that the generation of OTDZs was determined by the preferred nucleation of  $\gamma$  lamellae at high temperatures.

As shown in Fig. 4, the red lines defined as LAGBs denote grain boundaries with a misorientation between 2° and 10°. The LAGBs are obtained due to the substructures caused by thermal-induced deformation [21,22]. Only a few LAGBs are observed on CT<sub>1</sub> specimen, most of which are colony boundaries as shown in Fig. 4(a). Oppositely, a lot of LAGBs are observed on CT<sub>2</sub> specimen, which distribute heterogeneously on  $\gamma$  phase as shown in Fig. 4(b). The LAGBs concentrate on  $\gamma$  grains at colony boundaries and triple junctions, and distribute unevenly among different lamellar colonies. These findings indicate the

Download English Version:

<https://daneshyari.com/en/article/5457579>

Download Persian Version:

<https://daneshyari.com/article/5457579>

[Daneshyari.com](https://daneshyari.com)